Carbon Cycle Dynamics
For a Neoproterozoic
Climate Model

By

John Wilfrid Crowley

A THESIS SUBMITTED IN PARTIAL FULFILLMENT
OF THE REQUIREMENTS FOR THE DEGREE
OF BACHELOR OF APPLIED SCIENCE

DIVISION OF ENGINEERING SCIENCE

FACULTY OF APPLIED SCIENCE AND ENGINEERING
UNIVERSITY OF TORONTO

Supervisor: W.R. Peltier

April 12th, 2006

J. W. Crowley

Abstract:

The carbon cycle model of Rothman et al. [2003] is modified by allowing temperature dependent photosynthetic and remineralization fluxes and through the introduction of a temperature dependent photosynthetic isotopic fractionation. The carbon model is then coupled to the energy balance/ice-sheet model (EBM)/(ISM) of Peltier and Tarasov [1999]. Two major solutions are found. For a magnitude of the remineralization flux parameter of 0.0003 or less, a hysteresis loop forms in the temperature-dRad phase space with oscillations having a period controlled by the flux parameter and which can have glacial-interglacial timescales greater than 3Myr. When the magnitude of the remineralization flux parameter is greater than or equal to 0.0006, the system approaches an equilibrium state. There is a suggestion in the results of the simulation with the remineralization flux parameter set to 0.0006 that a Hard Snowball Earth state could exist for values of the flux parameter greater than 0.0006. Isotopic data for inorganic carbon is produced which matches data from the Neoproterozoic era remarkably well in both the complicated trajectory that exists in the inorganic carbon isotopic composition vs. photosynthetic isotopic fractionation phase plane and in the large scale variations of isotopic composition for inorganic carbon.

J. W. Crowley

J. W. Crowley

Table of Contents:

J. W. Crowley

List of Symbols:

Symbol	Definition
δ_a, $\delta^{13}C$, δ_1	Isotopic composition of inorganic carbon
δ_o, δ_2	Isotopic composition of organic carbon
$\dot{\delta}_a$, $\dot{\delta}^{13}C$	Rate of change of isotopic composition of inorganic carbon
$\dot{\delta}_o$	Rate of change of isotopic composition of organic carbon
M_1	Mass of inorganic carbon in model
M_2	Mass of organic carbon in model
τ_1	Time constant for inorganic carbon reservoir
τ_2	Time constant for organic carbon reservoir
$\dot{M}_1$	Rate of change of mass of inorganic carbon in model
$\dot{M}_2$	Rate of change of mass of organic carbon in model
δ_i	Average isotopic composition of carbon entering the system
μ	Ratio of the time constant of the inorganic carbon reservoir to the time constant of the organic carbon reservoir
J_i	Mass flux of carbon entering the system
b_1	Mass flux of carbon leaving the inorganic carbon reservoir as burial
b_2	Mass flux of carbon leaving the organic carbon reservoir as burial
f	Ratio of organic burial to total burial
ε_o	Average photosynthetic isotopic fractionation
ε	Temperature dependent photosynthetic isotopic fractionation
J_{12e}	Mass flux from inorganic carbon reservoir to organic carbon reservoir at equilibrium (Photosynthetic flux - Rothman model)
J_{21e}	Mass flux from organic carbon reservoir to inorganic carbon reservoir at equilibrium (Remineralization flux - Rothman model)
J_{12}	Temperature dependent mass flux from inorganic carbon reservoir to organic carbon reservoir (Photosynthetic flux - new model)
J_{21}	Temperature dependent mass flux from organic carbon reservoir to inorganic carbon reservoir (Remineralization flux - new model)
J_1	Total mass flux through inorganic carbon reservoir at equilibrium
J_2	Total mass flux through organic carbon reservoir at equilibrium
ϕ_{12}	Ratio of J_{12} to J_1 at equilibrium
O_{2sole}	Oxygen solubility of seawater at equilibrium
O_{2sol}	Temperature dependent oxygen solubility
T_e	Equilibrium temperature which reduces temperature dependent values to the steady state values of the Rothman model
T	Temperature
A	Constant of proportionality for linear approximation of oxygen solubility
B	Constant of proportionality for linear approximation of remineralization flux
F_{12}	Remineralization flux parameter
F_{21}	Photosynthetic flux parameter
$dRad$	Surface radiation balance due to atmospheric carbon dioxide
a_{frac}	Proportionality constant for linear temperature dependence of photosynthetic isotopic fractionation

J. W. Crowley

List of Figures and Tables:

While writing up the thesis an error in equation (28) was propagated through the equations. The following are corrections:

Equation (28)

$$J_{21} = J_{21_e}\left[1 + B\left(\frac{O_{2sol} - O_{2sol_e}}{O_{2sol_e}}\right)\right] = \left[\frac{M_{1_e}\phi_{12_e}}{\tau_1} - \left(\frac{f}{1-f}\right)\frac{M_{1_e}\left(1 - \phi_{12_e}\right)}{\tau_1}\right]\left[1 + B\left(\frac{O_{2sol} - O_{2sol_e}}{O_{2sol_e}}\right)\right]$$

Equation (29) and (32)

$$J_{21} = \frac{M_{1_e}}{\tau_1}\left[\phi_{12_e} - \left(\frac{f}{1-f}\right)\left(1 - \phi_{12_e}\right)\right]\left[1 - F_{21}(T - T_e)\right]$$

Equation (34)

$$\dot{\delta}_a = \left\{\frac{M_{1_e}(1 - \phi_{12_e})}{M_1\tau_1(1-f)}\right\}(\delta_i - \delta_a) + \left\{\frac{M_{1_e}}{M_1\tau_1}\left[\phi_{12_e} - \left(\frac{f}{1-f}\right)\left(1 - \phi_{12_e}\right)\right]\left[1 - F_{21}(T - T_e)\right]\right\}(\delta_o - \delta_a)$$

$$+ \left\{\left[\frac{M_{1_e}\phi_{12_e}}{M_1\tau_1}\right]\left[1 - F_{12}(T - T_e)\right]\right\}\left[\varepsilon_o - a_{frac}(T - T_e)\right]$$

Equation (36)

$$\dot{M}_1 = \frac{M_{1_e}}{\tau_1}\left[\frac{f - \phi_{12_e}}{1-f}F_{21} + \phi_{12_e}F_{12}\right](T - T_e)$$

Equation (37)

$$\dot{M}_2 = -\frac{M_{1_e}}{\tau_1}\left[\frac{f - \phi_{12_e}}{1-f}F_{21} + \phi_{12_e}F_{12}\right](T - T_e)$$

1. Introduction

1.1 Neoproterozoic Climate, Snowball Earth, and $\delta^{13}C$

One of the major driving forces behind the Snowball Earth hypothesis, the

suggestion that the Earth was once
entirely ice-covered, is the observed
large amplitude variability in del-13C
($\delta^{13}C$) measured in carbonate
sequences of the Neoproterozoic era.
The Neoproterozoic era spans from
roughly one billion years ago to
around 550 million years ago. Figure
1 shows the $\delta^{13}C$ time series of
Halverson et al. [2005] for most of
the Neoproterozoic era. It has been
suggested that the variability in the
$\delta^{13}C$ time series could have occurred
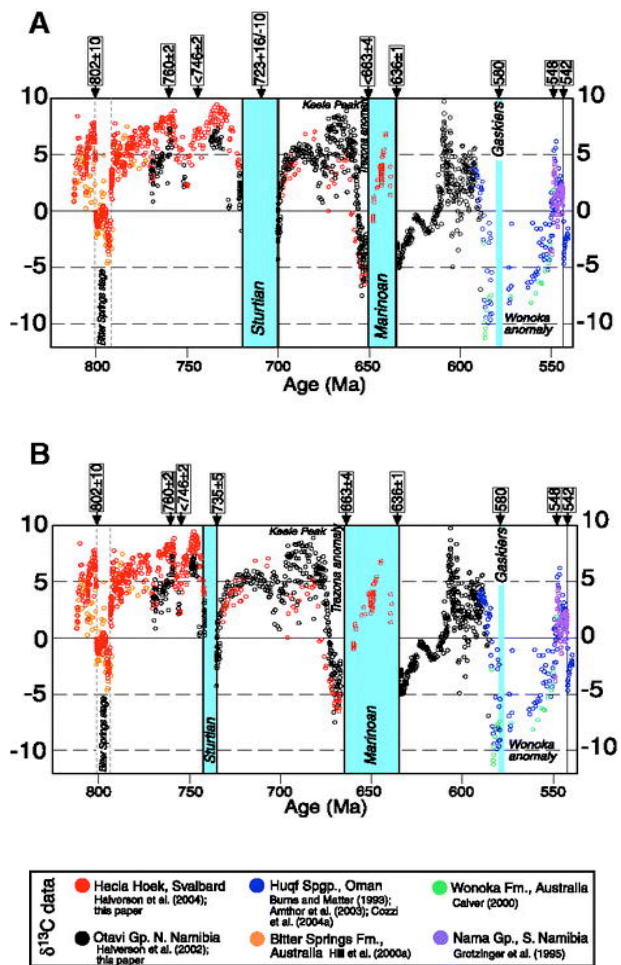if photosynthetic production had all
but nearly ceased.

*Figure 1: Two of the $\delta^{13}C$ time series
of Halverson et al. [2005]*

While several groups originally argued that photosynthetic life could have found

refuge during a Snowball Earth event at equatorial thin-ice regions where light could still

penetrate the thin ice (<10m) [eg. McKay, 2000], it was later shown that regions of thin ice could not survive at the equator due to crystallized brine pockets of salt which would alter the albedo and surface heat flux of the ice and also due to the intrusion of sea glaciers which would rip apart and destroy thin ice [Warren et al. 2002]. Thus the scenario of an ice encapsulated Earth would provide the necessary mechanism to halt photosynthetic production as little light would be able to penetrate the deep ice of the "Hard Snowball" like state and could have lead to the large amplitude variability depicted in figure 1.

However, the implications of a Hard Snowball event and the consequent halt of photosynthetic life which would follow is a source of major controversy as it seems to conflict with the history of biological evolution [eg. Runnegar, 2000; Knoll, 2003]. A study of the evolution of early life forms has shown that the ancestors of the biota involved in the "Cambrian Explosion of Life" had existed in the Neoproterozoic era as well in the form of eukaryotic life forms (algae). Had the earth entirely frozen over, thick ice would have ended most photosynthetic activity and likely also resulted in the extinction of species that required photosynthesis for survival and these life forms would not have been around to evolve.

Fortunately, an alternative to the Snowball Hypothesis was presented in a paper by Hyde et al. [2000] in which it was suggested that the most likely state of the climate system during Neoproterozoic time would be one in which the earth only partially froze over with open water still existing near the equator. This new solution has been named the "Oasis solution" or the "Slushball Earth" solution. While the Slushball Earth solution seems to avoid the pitfall of terminating photosynthetic life, it has been criticized on the

grounds that it is unable to produce the appropriate timescale between glacial and interglacial states (>~3Myr) [Schrag et al., 2001]. A further criticism of the Slushball solution is the claim that such solutions are unable to produce variations of the observed magnitude in the $\delta^{13}C$ time series.

This paper will demonstrate the importance and overall effect of the carbon cycle on Neoproterozoic climate dynamics and its affect on the timescales between glacial and interglacial events as well as its influence on $\delta^{13}C$ values.

1.2 The Neoproterozoic Carbon Model (The Rothman Model)

A Neoproterozoic model of the carbon cycle was constructed by Rothman et al. [2003] in which the carbon in the oceans and atmosphere was modeled as two reservoirs of constant mass; one for organic carbon and the second for inorganic carbon. The masses of the two reservoirs were assumed to be constant with the system operating at steady state. The model is shown in figure 2. The reservoir on the left represents the inorganic carbon with mass M_1, time constant τ_1, and isotopic composition δ_a (shown as δ_1). Similarly, the reservoir on the right represents the organic carbon with mass M_2, time constant τ_2, and isotopic composition δ_o (shown as δ_2). The symbols and subscripts are consistent with those used by Rothman. The isotopic composition is defined as

$$\delta_x = 1000\left(\frac{R_x - R_{STD}}{R_{STD}}\right) \quad \text{where} \quad R_x = \frac{^{13}C}{^{12}C} \quad \text{is the isotopic ratio for the sample.} \quad \delta_a \text{ is also}$$

commonly referred to as $\delta^{13}C$ (as in the discussion above).

Fluxes between reservoirs represent the photosynthetic flux as J_{12} (including isotopic depletion by an amount ϵ_o), and remineralization flux as J_{21}. Fluxes b_1 and b_2 out

of the reservoirs represent carbon burial. The flux J_i into the inorganic reservoir represents volcanic and other inputs with average isotopic content δ_i.
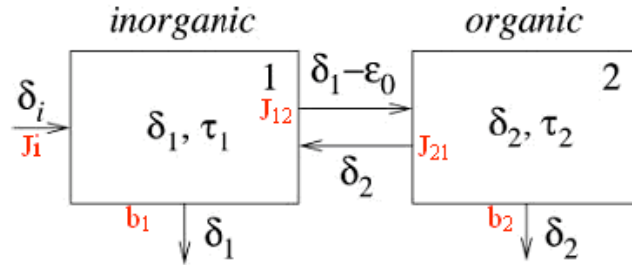
Figure 2: The Rothman Carbon Cycle. Figure as in Rothman et al. [2003]

By definition, J_1 and J_2 are the total mass fluxes into and out of the inorganic and organic carbon reservoirs respectively. Thus at equilibrium,

$$J_{1_e} = J_{12_e} + b_{1_e} \quad \text{and} \quad J_{1_e} = J_{i_e} + J_{21_e} \tag{1}$$

$$J_{2_e} = b_{2_e} + J_{21_e} \quad \text{and} \quad J_{2_e} = J_{12_e} \tag{2}$$

where the subscript *e* denotes an equilibrium value.

The time constants τ_1 and τ_2 are taken at steady state and are defined as

$$\tau_1 = M_{1_e} / J_{1_e} \tag{3}$$

$$\tau_2 = M_{2_e} / J_{2_e} \tag{4}$$

Other constants defined and used are the normalized photosynthetic flux, ϕ_{12}, defined as the ratio of the flux J_{12} to the flux J_1, the organic portion of the output as a fraction of the total output, f, and the ratio of the two time constants, μ. These values are given by:

$$\phi_{12} = J_{12} / J_1 \tag{5}$$

$$f = \frac{b_2}{(b_2 + b_1)} \tag{6}$$

$$\mu = \tau_1 / \tau_2 \tag{7}$$

The defining equations for the system presented by Rothman et al. are

$$\dot{\delta}_a = \frac{J_i}{M_1}(\delta_i - \delta_a) + \frac{J_{21}}{M_1}(\delta_o - \delta_a) + \frac{J_{12}}{M_1}\varepsilon \tag{8}$$

$$\dot{\delta}_o = \frac{J_{12}}{M_2}(\delta_a - \varepsilon - \delta_o) \tag{9}$$

$$\dot{M}_1 = J_i + J_{21} - J_{12} - b_1 \tag{10}$$

$$\dot{M}_2 = J_{12} - J_{21} - b_2 \tag{11}$$

For constant ϕ_{12_e}, the fluxes are constant in the Rothman model. Substituting the

first eq'n of (1) into (5) gives

$$\phi_{12_e} = \frac{J_{12_e}}{b_{1_e} + J_{12_e}} \tag{12}$$

From which it then follows that

$$J_{12_e} = \left(\frac{\phi_{12_e}}{1 - \phi_{12_e}}\right)b_{1_e} \tag{13}$$

Combining the first of eq'n (1) with eq'n (3) gives

$$M_{1_e} = \tau_1(b_{1_e} + J_{12_e}) \tag{14}$$

Substituting (13) into (14) and solving for b_1 gives

$$b_{1_e} = \frac{M_{1_e}(1 - \phi_{12_e})}{\tau_1} \tag{15}$$

Substituting the second eq'n of (2) into (4) and then substituting that and eq'n (3)

into (7) gives

5

$$\mu = \left(\frac{M_{1_e}}{M_{2_e}}\right)\left(\frac{J_{12_e}}{J_{1_e}}\right) \tag{16}$$

Now making use of eq'n (5) and solving for M_{2e} in (16) results in

$$M_{2_e} = \frac{\phi_{12_e} M_{1_e}}{\mu} \tag{17}$$

Equation (17) gives the equilibrium size of the organic carbon reservoir relative to the inorganic carbon reservoir.

Solving for b_2 in (6) and substituting in b_1 from (15) provides

$$b_{2_e} = \left(\frac{f}{1-f}\right)\frac{M_{1_e}(1-\phi_{12_e})}{\tau_1} \tag{18}$$

Adding eqn's (10) and (11) together at steady state (ie. $dM_1/dt=0$ and $dM_2/dt=0$) and solving for J_i gives

$$J_{i_e} = b_{1_e} + b_{2_e} \tag{19}$$

Substituting (15) and (18) into (19) results in

$$J_{i_e} = \frac{M_{1_e}(1-\phi_{12_e})}{\tau_1(1-f)} \tag{20}$$

Substituting eq'n (15) into (13) gives

$$J_{12_e} = \frac{M_{1_e}\phi_{12_e}}{\tau_1} \tag{21}$$

Using the first of eq'n (2) and substituting in eqn's (18) and (21) gives

$$J_{21_e} = \frac{M_{1_e}\phi_{12_e}}{\tau_1} - \left(\frac{f}{1-f}\right)\frac{M_{1_e}\left(1-\phi_{12_e}\right)}{\tau_1} \tag{22}$$

By introducing a time dependent sinusoidal value for ε and assuming that the mass of the organic reservoir was approximately one hundred times that of the organic,

Rothman et al. were able to reproduce phase curves in the δ_a vs. ε phase plane that resembled observational data.

1.3 The Energy Balance Model / Ice Sheet Model

The carbon cycle is coupled to an energy balance model (EBM) that is coupled to an ice sheet model (ISM).

The coupled EBM/ISM model was previously used to model climate dynamics related to the plausibility of the "snowball bifurcation" by Peltier and Tarsov [Peltier et al., 2004] as well as predicting the evolutionary history of the North American and Eurasian ice sheets over the last glacial cycle [Tarasov and Peltier, 1999, Peltier, 2002]. The global EBM is essentially that of North et al. [1983] to which has been added a full three dimensional thermomechanical ISM. The full model consists of several individual elements linked by nonlinear partial differential equations. The main component of the EBM is the nonlinear diffusion equation:

$$C(\bar{r},t)\frac{\partial T_s(\bar{r},t)}{\partial t} = \overline{\nabla}_h \cdot \left[D(\theta)\overline{\nabla}_h T_s\right] - (A + BT_s) + a(\bar{r},t)\frac{Q}{4}S(\theta,t) \qquad (23)$$

in which $C(\underline{r},\ t)$ is the space and time dependent heat capacity of the surface of the sphere which is used to differentiate continental from oceanic surface and ice covered from non-ice-covered surface. $D(\theta)$ is the diffusion coefficient which is latitude dependent, $T_s(\underline{r},\ t)$ is the time and space dependent surface temperature, and the values of A and B are associated with the black body emission of the earth. The space and time dependent function $S(\theta,\ t)$ represents the variation of the insulation incident at the top of the atmosphere which includes the change due to deviations in the parameters that correspond to the geometry of Earth's orbit around the Sun. The space and time

dependent parameter $a(r, t)$ is the surface albedo which is used to distinguish a highly reflective surface such as ice from less reflective surfaces such as continents. Q is the solar constant and is equal to approximately $1370 W/m^2$.

Modifying the coefficient A, provides a reduction or enhancement of the infrared forcing at the surface that arises from a change in the atmospheric carbon dioxide concentration. It is through the parameter A that the carbon cycle model is coupled to the EBM.

The EBM is coupled to a three-dimensional thermo-mechanical model of continental ice-sheet evolution. The central component of the ISM is the non-linear diffusion equation for ice thickness H which is given by equation (24).

$$\frac{\partial H}{\partial t} = -\nabla_h \cdot \int_{Z_b}^{h} \overline{V}(\overline{r})dz + G(\overline{r}, T(\overline{r})) \tag{24}$$

where

$$\overline{V}(\overline{r}) = \overline{V}_b(\overline{r}) - 2(\rho_i g)^m \left\{ \nabla_h(h) \cdot \nabla_h(h) \right\}^{(m-1)/2} \cdot \nabla_h(h) \cdot f \int_{Z_b}^{Z} A(T(z'))(h - z')^m dz' \tag{25}$$

in which h is the surface elevation above present-day sea level, ρ_i is the density of ice, g is the acceleration due to gravity, T is the temperature of the ice, and G is the net mass balance. Both (23) and (24) are solved on the surface of the sphere. In (24), the $A(T)$ is a term which represents the degree of crystalline anisotropy and/or impurities in the ice.

The final component of the ice-sheet coupled EBM consists of a model of the glacial isostatic adjustment (GIA) process represented by a simple "damped return to equilibrium" model that has the following form:

$$\frac{\partial h'}{\partial t} = \frac{(h'(\overline{r},t) - h_o(\overline{r},0))}{\tau} + \frac{\rho_i}{\rho_E} \frac{H}{\tau} \tag{26}$$

in which τ = 4kyr is the assumed constant relaxation time of the adjustment process, $h_o(\underline{r},\,0)$ is the topography with respect to sea level of the unglaciated state, ρ_i and ρ_E are the densities of ice and Earth respectively, and h is the vertical bedrock deflection due to loading.

A more detailed description of the EBM/ISM may be found in the cited references and thus further details are omitted here.

The EBM/ISM solves a spatially and time dependent problem in which surface temperature values for the earth, as well as ice cover for both land and sea, are variables among the solution set. The EMB/ISM computes a mean sea level temperature for a small increment of time which is passed to the carbon cycle model. The carbon cycle model then calculates the new temperature dependent fluxes and photosynthetic isotopic fractionation which it then uses to compute the new carbon reservoir sizes and their respective isotopic compositions. The carbon cycle model then passes the new atmospheric carbon dioxide concentration to the EBM/ISM which uses it to calculate a new mean sea level temperature for the earth. And consequently the models are coupled and interact through the time dependent values of temperature and atmospheric carbon dioxide concentration.

2. The New Model

2.1 Temperature-Dependent Mass Transport through Oxygen Solubility

Allowing mass transport between the two carbon reservoirs modifies Rothman's model and allows it to be used as a primitive method for predicting atmospheric carbon dioxide levels.

The main idea is that the remineralization flux should be temperature dependent. As mentioned in Rothman et al. [2003], as temperatures decrease, the solubility of oxygen in the ocean increases and surface waters become oxygen enriched. This oxygen enrichment increases the rate of oxidation of organic carbons, thus increasing the amount of inorganic carbon in the oceans. As the atmosphere equilibrates with surface waters on a short time scale (less than a thousand years), its concentration of carbon dioxide will increase as well.
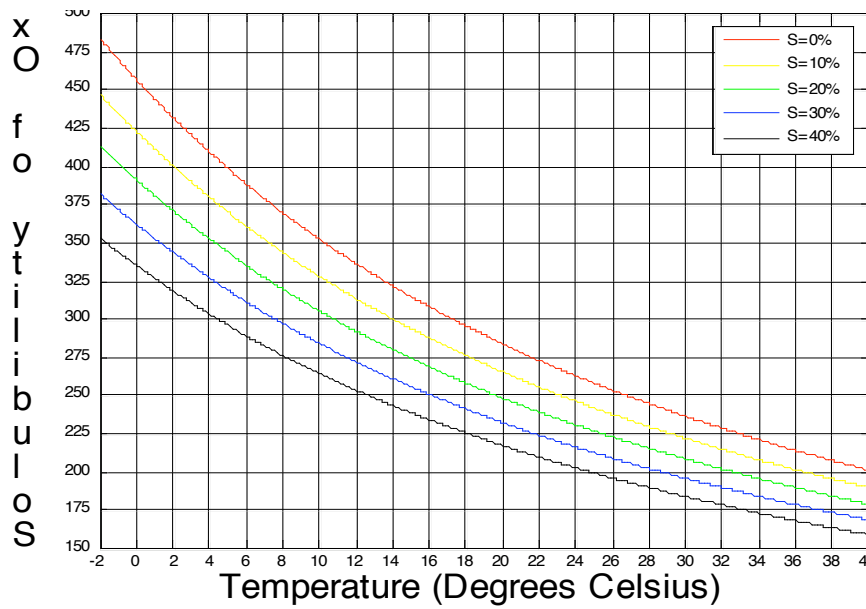

Figure 3: Oxygen Solubility as a Function of Temperature and Salinity

Figure 3 shows how the solubility of oxygen in salt water changes as a function of temperature. The solubility curves for oxygen were generated using the equations for oxygen solubility in seawater developed by Garcia et al. [1992]. The different curves shown are for various oceanic salinities.

In the revised carbon model a linear function is used to approximate the solubility of oxygen in the ocean as a function of temperature and is given by equation (27), where the e subscript denotes an equilibrium value at an equilibrium temperature T_e, and A is a constant.

$$O_{2sol} = O_{2sol_e} + A(T - T_e) \tag{27}$$

The remineralization flux is allowed to be linearly proportional to the oxygen solubility with an equilibrium flux of J_{21e} equal to that used in Rothman's model at an equilibrium temperature T_e. Away from equilibrium, the flux J_{21} is allowed to vary as a function of the oxygen solubility and is expressed by equation (28), with B as a constant.

$$J_{21} = \frac{M_{1_e} \phi_{12_e}}{\tau_1} \left[1 + B \left(\frac{O_{2sol} - O_{2sol_e}}{O_{2sol_e}} \right) \right] - \left(\frac{f}{1-f} \right) \frac{M_{1_e} (1 - \phi_{12_e})}{\tau_1} \tag{28}$$

Substituting equation (27) into equation (28) and letting $F_{21} = -AB/O_{2sol_e}$, equation (29) shows how J_{21} may be expressed explicitly as a function of temperature. Note that the sign of F_{21} will be positive by definition since A is expected to be negative (negative slope of oxygen solubility curve) and B and O_{2sole} are both positive values.

$$J_{21} = \frac{M_{1_e} \phi_{12_e}}{\tau_1} \left[1 - F_{21}(T - T_e) \right] - \left(\frac{f}{1-f} \right) \frac{M_{1_e} (1 - \phi_{12_e})}{\tau_1} \tag{29}$$

If the mass of the inorganic carbon reservoir increases beyond its regular steady state value then a similar argument could be made to increase the photosynthetic flux if

one desired. Thus for generality, the photosynthetic flux J_{12} will be allowed to vary as a function of temperature according to equation (30).

$$J_{12} = J_{12e}\left[1 - F_{12}(T - T_e)\right] \tag{30}$$

The photosynthetic and remineralization fluxes may be expressed as equations (31) and (32) after substituting in the steady state fluxes from equations (21) and (22) respectively.

$$J_{12} = \left[\frac{M_{1_e}\phi_{12_e}}{\tau_1}\right]\left[1 - F_{12}(T - T_e)\right] \tag{31}$$

$$J_{21} = \frac{M_{1_e}\phi_{12_e}}{\tau_1}\left[1 - F_{21}(T - T_e)\right] - \left(\frac{f}{1-f}\right)\frac{M_{1_e}\left(1 - \phi_{12_e}\right)}{\tau_1} \tag{32}$$

The inward and burial fluxes remain the same as in the Rothman model to ensure mass conservation for the entire system and are given by equations (15), (18), and (20).

2.2 Temperature-Dependent Isotopic Fractionation

A second critical change to the model which has no affect on mass transport but that does play an important role in the behavior of the isotopic composition is the added temperature dependence for the photosynthetic isotopic fractionation value ε. This relationship is justified on the grounds of several papers, including Wong and Sackett [1978], which suggest that the value for photosynthetic isotopic fractionation for certain species may vary as much as 0.4%/°C. A linear relationship will be used for the isotopic fractionation and is given by equation (33).

$$\varepsilon = \varepsilon_o - a_{frac}(T - T_e) \tag{33}$$

-8

2.3 Summary of Model

Using equations (15), (18), (20), (31), (32), and (33) for b_1, b_2, J_i, J_{12}, J_{21}, and ε respectively, and substituting them into equations (8) through (11) gives the time-dependent equations for the new system. They are:

$$\dot{\delta}_a = \left\{ \frac{M_{1_e}(1 - \phi_{12_e})}{M_1 \tau_1 (1-f)} \right\}(\delta_i - \delta_a) + \left\{ \frac{M_{1_e}\phi_{12_e}}{\tau_1}\left[1 - F_{21}(T - T_e)\right] - \left(\frac{f}{1-f}\right)\frac{M_{1_e}(1 - \phi_{12_e})}{\tau_1} \right\}(\delta_o - \delta_a)$$

$$+ \left\{ \left[\frac{M_{1_e}\phi_{12_e}}{M_1 \tau_1}\right]\left[1 - F_{12}(T - T_e)\right]\right\}\left[\varepsilon_o - a_{frac}(T - T_e)\right] \tag{34}$$

$$\dot{\delta}_o = \left\{ \left[\frac{M_{1_e}\phi_{12_e}}{M_2 \tau_1}\right]\left[1 - F_{12}(T - T_e)\right]\right\}(\delta_a - \left[\varepsilon_o - a_{frac}(T - T_e)\right] - \delta_o) \tag{35}$$

$$\dot{M}_1 = \frac{\phi_{12_e}(F_{12} - F_{21})(T - T_e)M_{1_e}}{\tau_1} \tag{36}$$

$$\dot{M}_2 = \frac{\phi_{12_e}(F_{21} - F_{12})(T - T_e)M_{1_e}}{\tau_1} \tag{37}$$

The model is completely described by specifying ϕ_{12_e}, μ, τ_1, ε_o, δ_i, a_{frac}, F_{12}, F_{21}, T_e, and f.

3 Experimental Setup:

3.1 The EBM/ISM:

All inputs to the EBM/ISM are the same as were used in Peltier et al. [2004]. The one exception being that the carbon dioxide concentration is variable and is determined by the coupled carbon cycle model.

The effect of carbon dioxide is expressed in the EBM/ISM as a deviation, in Watts per square meter, of the surface radiation balance due to a decrease or increase in atmospheric pCO_2, as in Peltier et al [2004], and is given by equation (38).

$$dRad = 5.35 \times \ln\left(\frac{C}{C_o}\right) \tag{38}$$

The parameter *dRad* is linearly proportional to the parameter *A* of equation (23) with a proportionality constant depending on Neoproterozoic conditions and described in Peltier et al. [2004].

If one assumes that the total amount of CO_2 in the system is some constant fraction, k_1, of the total amount of inorganic carbon, M_1, in the system, then

$$M_{CO_2 Tot} = k_1 M_1 \tag{39}$$

And if the amount of CO_2 expected to be in the atmosphere is some constant fraction, say k_2, of the total mass of CO_2, then

$$M_{CO_2 Atm} = k_2 M_{CO_2 Tot} \tag{40}$$

Equation (40) is clearly an approximation and an assumption of the model, as one would expect the partitioning of CO_2 between the atmosphere and the oceans to be temperature dependent due to the temperature dependence of CO_2 solubility. This model

J. W. Crowley

makes the assumption that the effect of the temperature dependent carbon dioxide solubility on the partitioning of CO_2 between the atmosphere and the ocean will be negligible compared to the effect of the change in atmospheric carbon dioxide resulting from the increase or decrease in the inorganic carbon reservoir size.

Furthermore, one may relate the partial pressure of CO_2 in the atmosphere, pCO_2, to the total mass of CO_2 in the atmosphere by another constant, say k_3

$$pCO_2 = k_3 M_{CO_2 Atm} \tag{41}$$

Combining (39) through (41) yields

$$pCO_2 = kM_1 \quad \text{with} \quad k = k_1 k_2 k_3 \tag{42}$$

If one takes the ratio of $pCO_2(t)$ (at some time t) to pCO_{2o} (where pCO_{2o} is some reference (or initial) atmospheric carbon dioxide partial pressure) then one obtains

$$\frac{pCO_2(t)}{pCO_{2_0}} = \frac{M_1(t)}{M_{1_0}} \tag{43}$$

For simplicity, the ratio of the instantaneous to reference (or initial) atmospheric mass of carbon dioxide is used rather than the ratio of the instantaneous to reference (or initial) atmospheric carbon dioxide concentration (in partial pressure).

3.2 The Carbon Cycle Model:

Several runs were completed in order to study the effect of changes in the parameters F_{21} and a_{frac} as well as running the model both synchronously and asynchronously.

The coupled model was run with the same parameter values as in Rothman's paper [2003]. The values used for the carbon model constants are given in table 1 on the

15

following page. Just as in Rothman's paper, the values of ϕ_{12_e} and μ produce an organic

reservoir roughly 100 times larger then the inorganic reservoir and result in isotopic

changes that are most obvious in the inorganic carbon reservoir's isotopic data. The

initial mass of the inorganic carbon reservoir used is somewhat arbitrary and does not

affect the dynamics of the problem in any way. This can be understood by noting where

the time dependent and initial mass terms enter into the equations of the system

(equations 34-37). The initial value chosen for the runs was 40,000 Gig tons and is a

rough estimate of the amount of inorganic carbon in the oceans today [Kump, 2004]. The

parameter T_e was help constant at 1.

Parameter	Description	Value	Units
τ_1	Inorganic Carbon Reservoir Time Constant	1000	Years
μ	Ratio of Time Constants	10^{-2}	Unitless
ε_0	Isotopic Fractionation	28%	Per mil
δ_i	Input Flux Isotopic Composition	-6%	Per mil
φ_{12}	Normalized photosynthetic flux	0.999	Unitless
f	Ratio of Organic Burial	0.3	Unitless
T_e	Equilibrium Temperature	1	Degrees Celsius
M_{1i}	Initial Mass of Inorganic Carbon	40000	Giga Tons
F_{12}	Flux parameter for photosynthetic flux	0	Unitless
F_{21}	Flux parameter for remineralization flux	Var*	Unitless
a_{frac}	Photosynthetic isotopic fractionation constant	Var*	Per mil/C^o

Table 1: Carbon Cycle Constants
Var* indicates values which are varied for different model runs

3.3 The Coupling of the Models:

The physical coupling of the carbon cycle model and the EBM/ISM was performed by a summer NSERC student, Julien Rioux, in the department of physics at the University of Toronto. The data used in the following results was produced by Julien through the use of the coupled model code.

4 Results:

4.1 Existence of a Hysteresis Loop

For the first run the values of F_{21} and a_{frac} were set to 0.0003 and 0.3 %/^{o}C (per mill) respectively and the model was run synchronously.

The output mean sea level temperature, atmospheric carbon dioxide concentration (dRad), and mass of the inorganic carbon reservoir are all shown as a function of time in figure 4. The temperature fluctuates between approximately -9 ^{o}C and 9 ^{o}C with a regular period of 2040 ± 40 Ka. The system tends to cool and warm very rapidly with periods of slower temperature change between extremes. This is likely due to positive feedback mechanisms in the EBM/ISM such as ice sheet-albedo feedback. Figure 5
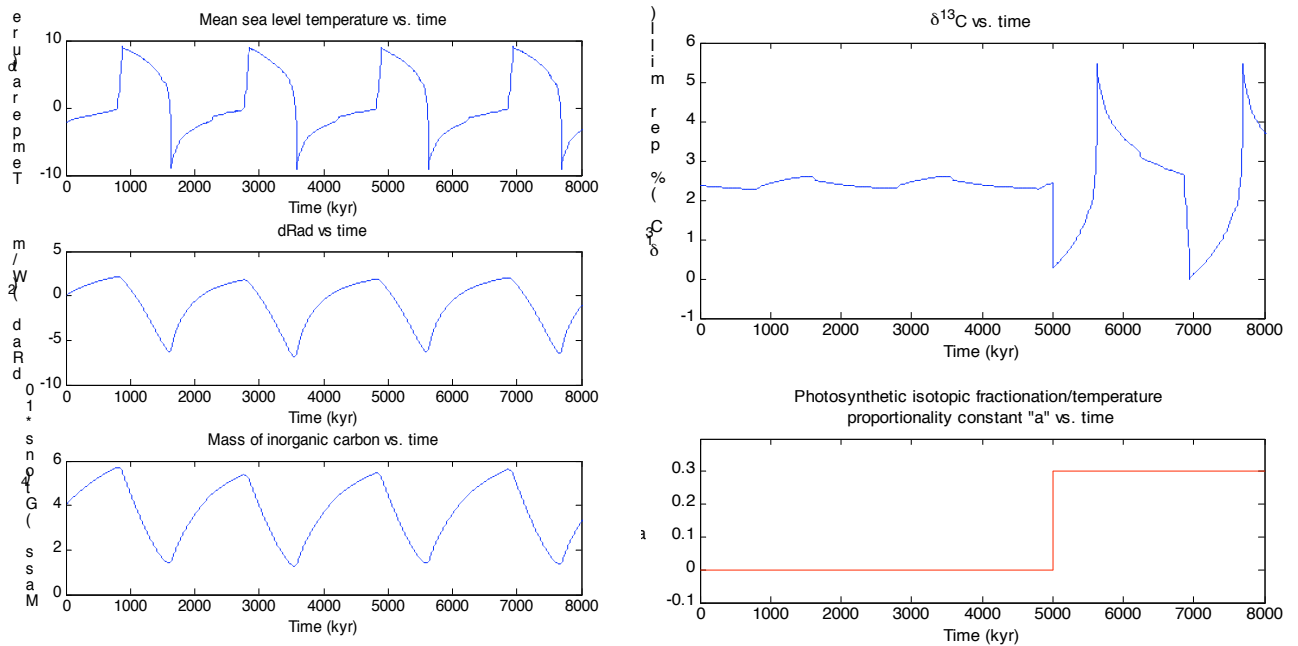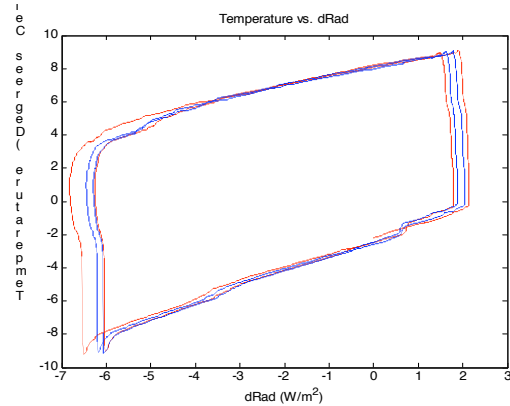

Figure 4: (Top) Mean sea level temperature vs. time, (Middle) Atmospheric carbon dioxide concentration (dRad) vs. time, (Bottom) Mass of carbon vs. time

Figure 5: (Top) $\delta^{13}C$ vs. time (Bottom) "a_{frac}" vs. time

shows both $\delta^{13}C$ and a_{frac} as functions of time in the model. The first 5Myr of simulation in figure 5 demonstrates that the $\delta^{13}C$ variations will be small as long as a_{frac} is set to zero. It is not until a_{frac} is set to 0.3 %/°C (per mill) that the variations in $\delta^{13}C$ become significant with respect to Neoproterozoic $\delta^{13}C$ variations.

Figure 6 shows the mean sea level temperature as a function of atmospheric carbon dioxide concentration (dRad). The red curve is for roughly the first four million years and the blue is for the remaining four million years of the simulation. The two colors show that the cycle is fixed and stable and figure 4 shows no evidence of the system drifting towards an equilibrium state.

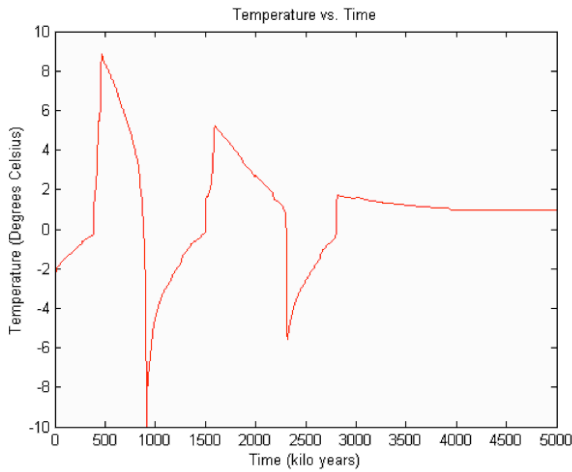*Figure 6: Mean sea level temperature vs. atmospheric carbon dioxide concentration (dRad)*

4.2 Existence of a Steady State Solution:

A second synchronous run with F_{21} set to 0.0006 and a_{frac} again at 0.3 %/°C (per mill) behaved quite differently from the previous run with no stable cycle existing and the system moving towards a steady state.

Figures 7 and 8 show the mean sea level temperature and the mass of the inorganic carbon reservoir, both as functions of time. Figure 9 displays both mean sea level temperature and the inorganic carbon reservoir size on the same plot to show the relative phases of the two. Both figures 7 and 8 show that the system relaxes to a steady state and figure 9 displays how the phase difference between the maximums in reservoir

mass and temperature decrease as time progresses. With the magnitude of F_{21} doubled from the previous run, it seems that the system is now able to exchange carbon between the reservoirs fast enough that the carbon cycle is able to stabilize the entire system. In other words, the carbon cycle "catches" up with the climate model.

It should also be noted that the period of the oscillations is approximately half that of the previous run and this seems to suggest that the period is strongly dependent on the value of the parameter F_{21}.

Figure 7: Mean sea level temperature vs. time
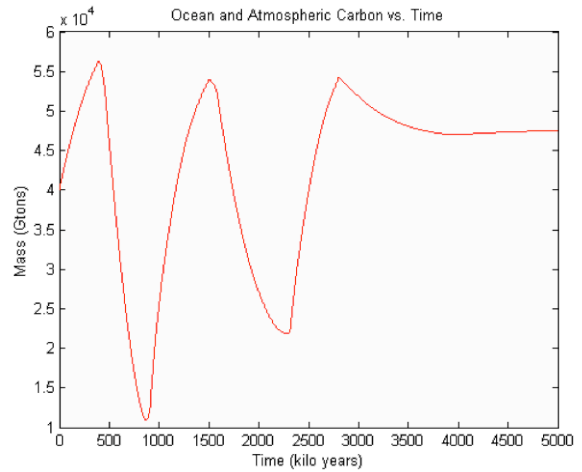
Figure 8: Mass of inorganic carbon vs. time
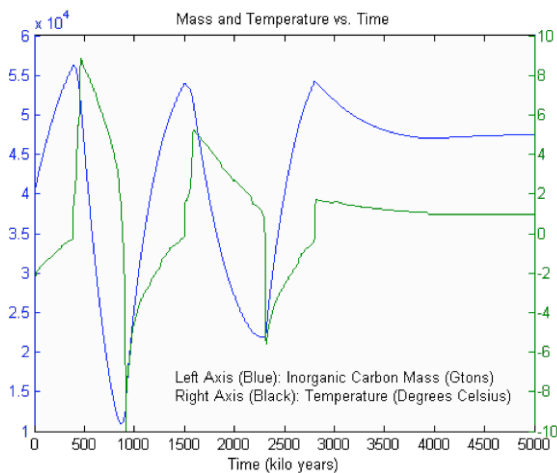
Figure 9: Mass of inorganic carbon and mean sea level temperature vs. time

Figure 10: Mean sea level temperature vs. atmospheric carbon dioxide concentration (dRad)

Figure 10 shows the same type of temperature vs. atmospheric carbon dioxide concentration plot as was given in figure 6 for the 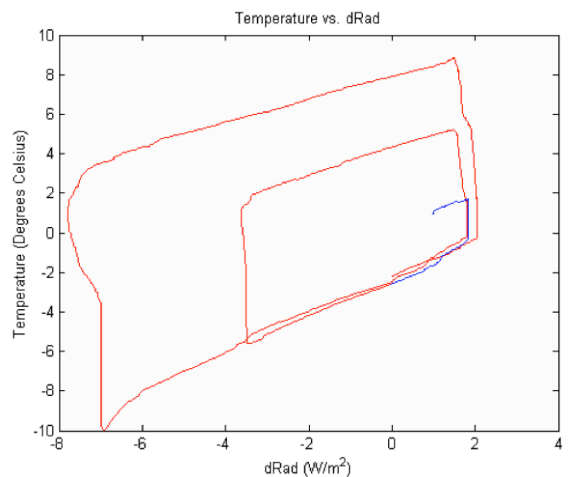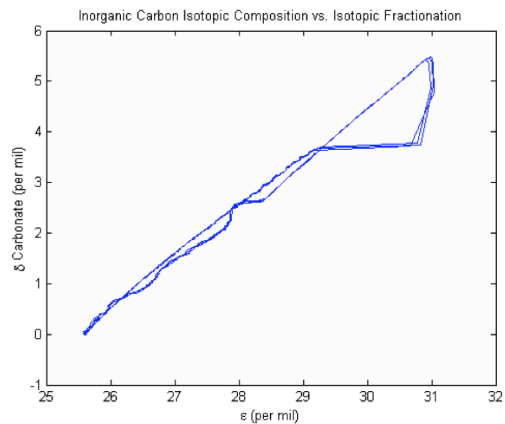first run. Again, the red curve is for the first half of the simulation in time and the blue curve for the second half. Figure 10 shows how the system behaves as it approaches its equilibrium state. The large path of the red curve and the short path of the blue curve illustrate how the dynamics of the system slow down as equilibrium is achieved.

An additional important observation taken from figure 10 is the apparent overshoot that the system makes as it descends along the "hot" upper branch of the hysteresis loop for the first time. Comparing the hysteresis loop of figure 10 to that of 6 shows that while the right side of the loops are close to identical, the lower left corner of the loop in figure 10 reaches both a lower temperature and a lower value of dRad than that of figure 6.

4.3 Behavior of the Carbon Isotopic Composition:

Setting the parameter a_{frac} to 0.3 %/^{o}C (per mill) provides a very promising result that strengthens the validity of the model. The isotopic fractionation ε varies as a function of temperature as described by equation (30) and affects the isotopic compositions of both the organic and inorganic carbon

Figure 11: Isotopic composition of inorganic carbon vs. the temperature dependent isotopic fractionation

reservoirs as mass is exchanged. The inorganic carbon reservoir is affected to a greater

extent due to its relatively smaller size. The effect may be seen in figure 11, which shows the isotopic composition of the inorganic reservoir, δ_a, as a function of the isotopic fractionation ε. The resulting relationship is a complex yet well behaved cycle. Figure 11 comes from the F_{21} = 0.0003 synchronous run and spans a time of approximately 6.5 million years, traversing just over 3 complete cycles.

### *4.4 Running the Model Asynchronously:*

Only one asynchronous run was attempted, as it was not completely successful. The values for F_{21} and a_{frac} were again 0.0003 and 0.30 %/°C (per mill) respectively. The model was run with the carbon cycle module time stepping at intervals of 1,000 years and the EBM/ISM stepping at intervals of 10,000 years.

Figure 12 compares the result of the mass of the inorganic carbon reservoir of the asynchronous run with that of the synchronous run with the same parameter settings.

The asynchronous run was found to evolve slower than that of the synchronous one.

It has not yet been determined if this result is due to problems with the forward solver or an issue with the time stepping.

It is expected that the system should be able to be run asynchronously since the carbon cycle evolves much slower than that of the EBM/ISM. The asynchronous trials are still being developed.
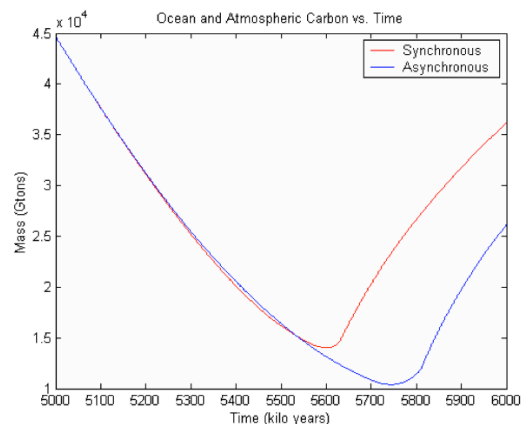
Figure 12: Inorganic carbon reservoir mass for synchronous and asynchronous runs

5 Discussion:

5.1 Overall effect of the Carbon Cycle on the Solution:

While the carbon cycle is simple in design, Rothman has validated its results at steady state and its new behavior with the addition of mass transport is entirely plausible.

Temperature dependent mass transport in the model introduces a mechanism for the carbon-cycle/EBM/ISM to behave in either a cyclic fashion or to approach an equilibrium state. A time dependent flux parameter, F_{21}, can allow the system to move back and forth between the two types of behavior.

The two synchronously run trials with differing values of F_{21} demonstrate that the period of oscillation in the climate system is heavily dependent on the carbon cycle and as such may be controlled by changing the flux parameter. Thus reducing F_{21} by a factor of ten would allow for "ice ages" with periods approximately ten times longer.

As the isotopic data will oscillate with a period equal to the period of oscillations of the carbon reservoirs mass, the coupled model can be made to produce data that fits the somewhat cyclic data of the Neoproterozoic era. Due to computational burden, runs of hundreds of millions of years of simulation time with $F_{21} << 0.0003$ could not be attempted.

For F_{21} values of 0.0003 and lower the system was locked in a stable limit cycle and evolved at a rate (and with a period) determined by the magnitude of F_{21}. Figure 6 may be compared with the hysteresis loop of Peltier et al. [2004] that was a solution for steady states using the same EBM/ISM described above. Observation shows that the two

solutions are in agreement and that the Earth would not enter into a "Hard Snowball" state for $F_{21} \leq 0.0003$.

For F_{21} values equal to or greater than 0.0006, the solution is quite different. The system settled to an equilibrium state and broke away from the cyclic climate behavior. The systems overshoot on its first descent along the "hot" branch of the hysteresis loop seems to suggest a rather important possibility; that the system may in fact be capable of much colder conditions due to the "momentum" of the system. The larger value of F_{21} allows the reservoirs to exchange mass at an increased rate. If the exchange of mass is rapid enough it may be possible for the entire system to be "thrown" off of the hysteresis loop and into a much colder state, as is partially demonstrated by figure 10. This result could demonstrate that this model is capable of displaying both "Snowball" and "Slushball" behavior for different values of the remineralization flux parameter F_{21}.

For some F_{21} value between 0.0006 and 0.0003 the system moves from its stable limit cycle to an equilibrium state. This result places an upper bound on the length of time it would take for the Earth to exit from the "ice age cycles" to a more steady state. Thus the upper bound is the period of approximately 2 million years, obtained from the $F_{21} = 0.0003$ run.

If the system were in a state with a flux parameter value less than 0.0003, it would be forced to oscillate between extreme warm and cold climates with a period dictated by the influence of oxygen solubility and the carbon cycle and a temperature magnitude bounded by the upper and lower bounds of the hysteresis loop. If something in the system's carbon cycle dynamics changed, the flux parameter would also be expected to change and could cause the system to exit from the cyclic pattern, potentially overshoot

the hysteresis loop and end up in some cold state, and then move to a more stable climate behavior.

The introduction of evolving multi-cellular organisms with organic carbon rich protective exoskeletons at the Precambrian explosion of life would no doubt have had a profound effect on the carbon cycle through their alteration of the remineralization flux parameter. This could account for the apparent change in the behavior of the $\delta^{13}C$ value at the end of the Neoproterozoic and would be entirely consistent with isotopic data for the Neoproterozoic and Precambrian eras.

5.2 Isotopic Behavior:

Just as the magnitude of the flux parameter may be changed to scale the behavior of the system in time, the constant a_{frac} in equation 16 for the isotopic fractionation may also be changed to alter the scale of the isotopic results.

As mentioned above, by introducing a time dependent sinusoidal value for ε and assuming that the mass of the organic reservoir was approximately one hundred times that of the organic, Rothman et al. were able to reproduce phase curves in the δ_a vs. ε phase plane that resembled observational data. Figure 13, taken from Rothman et al. [2003], shows isotopic data for the Neoproterozoic era from 738-549 million years ago. The data has several close similarities to the results shown in figure 11.

To begin with, the shape of the trajectory in figure 11 agrees with the Neoproterozoic data well. The broad upper end and thin elongated bottom of the loop in
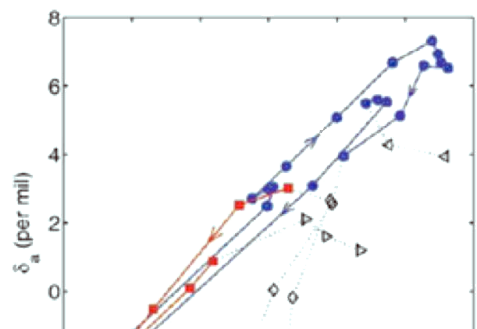
figure 11 seem to match the isotopic data well and appear a much better fit than the simple ellipsoid solutions of Rothman et al. [2003].

Figure 13: Trajectories in the del-13C vs. ε phase plane. Arrows indicate the forward direction in time which spans from 738Myr to 549Mry ago. Figure reproduced from Rothman et al. [2003]

Although the scales do not match, simply doubling a_{frac} would allow both the isotopic fractionation and the inorganic isotopic composition to deviate from their steady state values by as much as twice their present amounts. By adjusting ε_o and δ_i in the model, one can effectively translate the resulting image in the $\delta^{13}C$ vs. ε phase space. And furthermore, changing the magnitude of F_{21} would allow for the results to match the data on similar time scales (as discussed above). Thus varying the model parameters should produce highly agreeable results to the observationally determined Neoproterozoic data. And through finding the values of the parameters which produce the highest level of agreement between simulation and observational data, it will also be possible to infer a great deal about Neoproterozoic conditions such as the average photosynthetic isotopic fractionation and the degree of its temperature dependence.

Here it is important to note that it is primarily the change in the isotopic fractionation due to temperature dependence, occurring simultaneously with the mass transport, which causes the large scale $\delta^{13}C$ variations, and not the mass transport alone. This point is made clear by figure 5. As a result of the $\delta^{13}C$ results from the model being highly sensitive to the value of a_{frac}, a thorough investigation of Neoproterozoic life forms and their photosynthetic activity should be undertaken to explore the possible and acceptable values which may be used for further Neoproterozoic simulations.

This solution thus provides a mechanism for producing large $\delta^{13}C$ variations in a Neoproterozoic environment without having to resort to the "Hard Snowball Earth" solution and the implied limitations to photosynthetic life that accompany it.

While a greater analysis of the system would be beneficial to increasing our understanding regarding the threshold value of F_{21} which separates the equilibrium solution of figure 10 from the cyclic solution of figure 6, the possible existence of the Snowball solution in the model, the exact relationship between the value of F_{21} and the period of oscillations, and the actual degree of fit that one can obtain for the isotopic data, the program is rather temperamental and further work is required before additional simulations may be attempted.

6 Conclusions:

The carbon cycle model of Rothman et al. [2003] was modified by allowing the photosynthetic and remineralization fluxes to be temperature dependent as well as by introducing a temperature dependent photosynthetic isotopic fractionation.

The result of coupling the new carbon cycle model to an EBM/ISM was to produce a hysteresis loop in the temperature vs. dRad phase space that is consistent with the equilibrium solutions of Peltier and Tarasov [2004] for a remineralization flux parameter value of 0.0003 or less. This is a direct result of the EBM/ISM reacting faster than the carbon cycle.

The magnitude of the remineralization flux parameter was found to be inversely proportional to the period of the oscillations for the solutions with a hysteresis loop. Thus by decreasing the magnitude of F_{21}, oscillations that occur on time scales much longer than one or two million years can be easily achieved without changing the behavior of the system. Again, this is a direct result of the carbon cycle evolving slower than the EBM/ISM. This demonstrates that the Oasis/Slushball solutions can indeed produce glacial-interglacial timescales greater than 3Myr.

It was also observed that when the magnitude of the remineralization flux parameter was set greater than or equal to 0.0006, the carbon cycle was able to exchange mass fast enough to stabilize the entire Carbon/EBM/ISM model and an equilibrium state was achieved. The simulation results also suggested the possible existence of a colder Snowball-like state for values of F_{21} greater than 0.0006.

The threshold value for the remineralization flux parameter that yields a cyclic solution rather than a steady-state solution is known to be between 0.0003 and 0.0006.

Isotopic data for inorganic carbon was produced that matched Neoproterozoic data well by allowing the isotopic fractionation to vary as a linear function of temperature. It was found that a temperature dependent mass transfer alone could not produce large $\delta^{13}C$ variations but, when coupled to a temperature dependent photosynthetic isotopic fractionation, large deviations in $\delta^{13}C$ can occur. The shape of the cycle produced in the inorganic carbon isotopic composition vs. isotopic fractionation phase plane had remarkable similarities to the actual Neoproterozoic data that did not show up in the simulations and results produced by Rothman et al. [2003].

The results of this paper thus demonstrate that the model produces Oasis solutions that are in fact capable of producing large scale $\delta^{13}C$ variations of the historically observed magnitudes. An additional result is that the model may also be capable of producing Snowball events for large values of F_{21}. It is therefore important that a further study be undertaken to explore the acceptable range of values of F_{21} which may be used in the model.

Asynchronous runs were attempted but were not successful. An investigation into running the model asynchronously is currently taking place, and once complete, the carbon cycle model will be coupled and run asynchronously with a more detailed GCM such as the Community Climate System Model (CCSM) of the US National Center for Atmospheric Research (NCAR). These simulations will be required to further verify the existence of the hysteresis loop as well as the results of this paper.

6 References:

Garcia, H. E., and L. I. Gordon, Oxygen solubility in seawater: better fitting equations. *Limnol. Oceanogr.,* 37(6), 1307-1312, 1992.

Halverson, G. P., P. F. Hoffman, D. P. Schrag, A. C. Maloof, A. H. N. Rice, Toward a Neoproterozoic composite carbon-isotope record, *Geological Society of America Bulletin 117 (9-10):* 1181-1207, Sep-Oct 2005.

Hyde, W. T., T. J. Crowley, S. K. Baum., and W. R. Peltier, Neoproterozoic 'snowball Earth' simulations with a coupled climate/ice-sheet model, *Nature*, 405, 425-430, 2000.

Kump, R. K., J. F. Kastin, and R. G. Crane, The Earth System, Pearson Education, Inc, Upper Saddle River, New Jersey, 2004.

McKay, C. P., Thickness of tropical ice and photosynthesis on a snowball Earth, *Geophys. Res. Lett.*, 27, 2153-2156, 2000.

North, G. R., J. G. Mengel and D. A. Short, Simple energy balance climate model resolving the seasons and continents: Application to the astronomical theory of ice ages, *J. Geophys. Res*., 88, 6576-6586, 1983.

Peltier, W. R., Earth system history, In M. C. MacCracken and J. S. Perry (eds.), *The Encyclopedia of Global Environmental Change: vol. 1*, pp. 31-60, 2002.

Peltier, W. R., Tarasov, L., Vettoretti, G., and Solheim, L. P., Climate Dynamics in Deep Time: Modelling the "Snowball Bifurcation" and assessing the plausibility of its' occurrence. In The Extreme Proterozoic: Geology, Geochemistry, and Climate, Gregory Jenkins et. al. eds., *AGU Geophysical Monograph Series Volume 146*, pp 107-124, 2004.

Rioux, J. Effects of a carbon cycle box model on Neoproterozoic climate simulations, *Summer NSERC project, Dept. of Physics, University of Toronto*, 2005.

Rothman, D. H., J. M. Hayes, R. E. Summons, Dynamics of the Neoproterozoic carbon cycle, *Proceedings of the National Academy of Sciences of the United States of America 100 (14):* 8124-8129, 2003.

Schrag, D. P., and P. F. Hoffman, Life, geology, and snowball Earth, *Nature*, 409, 306, 2001.

Tarasov, L. and W. R. Peltier, Impact of thermomechanical ice sheer coupling on a model of the 100 kyr ice age cycle, *J. Geophys. Res.*, 104, 9517-9545, 1999.

Warren, S. G., R. E. Brandt, T. C. Grenfell, and C. P. McKay, Snowball Earth: Ice thickness on the tropical ocean, *J. Geophys. Res.*, 107, 3167-3184. 2002.

Wong, W. W., and W. M. Sackett, Fractionation of stable carbon isotopes by marine phytoplankton, *Geochim Cosmochum. Acta* 42, 1809-1815, 1978.